

## Caffeine consumption attenuates neurochemical modifications in the hippocampus of streptozotocin-induced diabetic rats

João M. N. Duarte,<sup>\*,†</sup> Rui A. Carvalho,<sup>\*,‡</sup> Rodrigo A. Cunha<sup>\*,§</sup> and Rolf Gruetter<sup>†,¶</sup>

<sup>\*</sup>Center for Neuroscience and Cell Biology, University of Coimbra, Coimbra, Portugal

<sup>†</sup>Laboratory for functional and metabolic imaging (LIFMET), Center for Biomedical Imaging (CIBM), Ecole Polytechnique Fédérale de Lausanne (EPFL), Lausanne, Switzerland

<sup>‡</sup>Department of Biochemistry, Faculty of Sciences and Technology, University of Coimbra, Coimbra, Portugal

<sup>§</sup>Institute of Biochemistry, Faculty of Medicine, University of Coimbra, Coimbra, Portugal

<sup>¶</sup>Departments of Radiology, University of Geneva and University of Lausanne, Lausanne, Switzerland

### Abstract

Type 1 diabetes can affect hippocampal function triggering cognitive impairment through unknown mechanisms. Caffeine consumption prevents hippocampal degeneration and memory dysfunction upon different insults and is also known to affect peripheral glucose metabolism. Thus we now characterized glucose transport and the neurochemical profile in the hippocampus of streptozotocin-induced diabetic rats using *in vivo* <sup>1</sup>H NMR spectroscopy and tested the effect of caffeine consumption thereupon. We found that hippocampal glucose content and transport were unaltered in diabetic rats, irrespective of caffeine consumption. However diabetic rats displayed alterations in their hippocampal neurochemical profile, which were normalized upon restoration of normoglycaemia, with the exception of *myo*-inositol that remained increased (36 ± 5%, *p* < 0.01 compared to controls) likely reflecting osmolarity deregulation. Compared to controls, caffeine-consuming diabetic rats displayed increased hippocampal levels of *myo*-inositol (15 ± 5%,

*p* < 0.05) and taurine (23 ± 4%, *p* < 0.01), supporting the ability of caffeine to control osmoregulation. Compared to controls, the hippocampus of diabetic rats displayed a reduced density of synaptic proteins syntaxin, synaptophysin and synaptosome-associated protein of 25 kDa (in average 18 ± 1%, *p* < 0.05) as well increased glial fibrillary acidic protein (20 ± 5%, *p* < 0.05), suggesting synaptic degeneration and astrogliosis, which were prevented by caffeine consumption. In conclusion, neurochemical alterations in the hippocampus of diabetic rats are not related to defects of glucose transport but likely reflect osmoregulatory adaptations caused by hyperglycemia. Furthermore, caffeine consumption affected this neurochemical adaptation to high glucose levels, which may contribute to its potential neuroprotective effects, namely preventing synaptic degeneration and astrogliosis.

**Keywords:** caffeine, diabetes, glucose, hippocampus, nuclear magnetic resonance, streptozotocin.

*J. Neurochem.* (2009) **111**, 368–379.

Diabetes mellitus has negative impacts on the central nervous system leading to diabetic encephalopathy and concomitant augmented incidence of cognitive problems (Brands *et al.* 2005), which are particularly associated with atrophy of the hippocampal formation that is involved in learning and memory processing (Convit *et al.* 2003; Gold *et al.* 2007). The frequently used model of type 1 diabetes, streptozotocin (STZ)-induced diabetic rats, is characterized by chronic hyperglycemia associated with impaired hippocampal-dependent learning and memory as well as defective synaptic plasticity in the hippocampus (Biessels *et al.* 1996). The

Received June 10, 2009; revised manuscript received July 16, 2009; accepted July 24, 2009.

Address correspondence and reprint requests to João M. N. Duarte, EPFL SB IPMC LIFMET (Bâtiment CH), Station 6, CH-1015 Lausanne, Switzerland. E-mail: joao.duarte@epfl.ch

**Abbreviations used:** BBB, blood-brain barrier; GFAP, glial fibrillary acidic protein; GLUT, glucose transporter; MAP2, microtubule-associated protein type 2; PSD95, post-synaptic density protein of 95 kDa; SNAP25, synaptosome-associated protein of 25 kDa; STZ, streptozotocin; TBS-T, Tris-buffered saline containing 0.1% Tween 20.

mechanisms linking diabetes to dysfunction of brain circuits are still unclear. One possibility is that hyperglycemia is responsible for deregulation of brain metabolism involving inadequate glucose utilization, which is the hallmark of diabetic conditions in peripheral tissues. However, published studies report inconsistent effects of hyperglycemia on substrate transport into the brain. In particular, glucose transport into the brain was suggested to be reduced (McCall *et al.* 1982), augmented (Duelli *et al.* 2000) or unaffected (Simpson *et al.* 1999) by chronic hyperglycemia. A second possibility to explain hyperglycemia-induced hippocampal dysfunction and damage resides in the disruption of osmotic balance, which is of fundamental importance for the viability of cells, in particular of neurons (Tomlinson and Gardiner, 2008).

As important as understanding the mechanisms linking diabetes to memory dysfunction is devising novel strategies to alleviate diabetes-induced memory impairment, which may also shed light on key mechanistic processes. A likely candidate is caffeine as chronic caffeine consumption abrogates memory impairment upon different insults (Cunha 2008; Takahashi *et al.* 2008) and affords robust neuroprotection (Cunha 2005; Chen *et al.* 2007). These effects are mimicked by antagonists of adenosine A<sub>2A</sub> receptors, which are the main molecular targets of chronic caffeine consumption (Fredholm *et al.* 1999). Adenosine receptors can control neuronal metabolism (Hammer *et al.* 2001) and osmolarity perturbations in the brain (Hada *et al.* 1998; Wurm *et al.* 2008), which may occur upon chronic hyperglycemia (see above). Furthermore, the observation that the density of A<sub>2A</sub> receptors is increased in the hippocampus of STZ-induced diabetic rats (Duarte *et al.* 2006) bolsters the interest of exploring the potential of chronic caffeine consumption to mitigate central diabetic encephalopathy.

The first aim of the present work was to determine the effect of a diabetic condition characterized by chronic hyperglycemia on the transport of glucose across the blood-brain barrier (BBB) and on the neurochemical profile in the hippocampus. The second aim was to determine if chronic caffeine consumption affects metabolic alterations in the hippocampus of STZ-induced diabetic rats. This was achieved using high-field *in vivo* NMR spectroscopy, which allows reliably measuring many metabolite concentrations that compose the neurochemical profile (Mlynárik *et al.* 2006) and quantify glucose uptake in hippocampal tissue. The final aim is to test if caffeine consumption could also counteract morphological features of neurodegeneration in the hippocampus of diabetic rats. In fact, chronic hyperglycemia triggers synaptic degeneration in the hippocampus of STZ-induced diabetic animals, in particular decreasing the density of synaptic proteins (Duarte *et al.* 2006; Grillo *et al.* 2005; Malone *et al.* 2006), and causes astrocyte reactivity and proliferation (Baydas *et al.* 2003; Saravia *et al.* 2002). Thus, we tested if long-term caffeine consumption might also

prevent synaptic alterations and astrogliosis induced by chronic hyperglycemia in the hippocampus of STZ-treated rats.

## Methods

### Animals

All experimental procedures involving animals were approved by the local ethics committee. Type 1 diabetes mellitus was induced in male Sprague–Dawley rats (8 weeks old, obtained from Charles River Laboratoires, Lentilly, France) by intra-peritoneal injection of STZ (65 mg/kg, prepared in sodium citrate buffer 10 mM, pH 4.5), which resulted in blood glucose levels above 300 mg/dL after 3 days as in previous studies (see Duarte *et al.* 2006) upon weekly measuring pre-prandial glycaemia from tail blood, using a glucometer based on the glucose oxidase method (Ascencia Contour, Bayer, Switzerland). Rats were maintained for 4 weeks with food and water *ad libitum*, and the NMR study was carried out 30 days after STZ-treatment, when sustained and chronic hippocampal alterations are observed (Alvarez *et al.* 2009; Duarte *et al.* 2006). Sham-treated age-matched control rats received vehicle injection and were maintained in the same conditions. Half of the animals were allowed to consume caffeine that was administered in the drinking water at 1 g/L for a period of 6 weeks starting 2 weeks before STZ administration. Because of polydipsia, STZ-induced diabetic rats received variable caffeine concentration to achieve similar caffeine consumption levels. Thus, in this experimental design we have four animal groups: control, caffeine-treatment, STZ-treatment, and STZ plus caffeine-treatment. Both body weight and caffeine consumption were monitored throughout the treatment period.

For the NMR studies, animals were anaesthetized using 2% isoflurane (Attane, Minrad, NY, USA) in oxygen gas for surgery, and then intubated and ventilated with a pressure-driven ventilator (MRI-1, CWE incorporated, Ardmore, PA, USA). Catheters were inserted into the femoral artery for monitoring blood gases, glucose and arterial blood pressure, and into the femoral vein for infusion of  $\alpha$ -chloralose (Acros Organics, Geel, Belgium), D-glucose (Sigma-Aldrich, Basel, Switzerland) and insulin (Humulin Normal, Eli Lilly, Switzerland). A blood sample (200  $\mu$ L) was collected and the serum was separated by centrifugation and stored for quantification of insulin and caffeine.

Animals were immobilized in a home-built holder with a bite bar and two ear inserts to minimize potential motion. Body temperature was maintained at 37.5°C with a warm water circulation system based on the feedback obtained from a rectal temperature probe. Arterial blood pressure, heart rate and respiratory rate were continuously monitored with an animal monitoring system (SA Instruments, Stony Brook, NY, USA). Before inserting the animal in the bore of the magnet, anesthesia was switched to  $\alpha$ -chloralose (intravenous bolus of 80 mg/kg and continuous infusion rate of 25 mg/kg/h). Insulin (0.5 U/mL solution) and D-glucose [20% (w/v) solution] were infused at a rate adjusted based on concomitantly measured arterial plasma glucose concentrations to achieve stable target glycaemia levels. NMR measurements were performed after each glucose level had been stable for more than 15 min. Arterial pH and pressures of O<sub>2</sub> and CO<sub>2</sub> were measured using a blood gas analyzer (AVL Compact 3, Diamond Diagnostics, Holliston, MA,

**Table 1** Physiologic parameters were maintained constant at the different ranges of plasma glucose concentration during the NMR experiment

	Body temperature (°C)	Arterial pH	P <sub>a</sub> CO <sub>2</sub> (mm Hg)
Control	37.5 ± 0.1	7.35 ± 0.01	42.0 ± 1.3
Caffeine	37.5 ± 0.1	7.35 ± 0.02	44.1 ± 3.6
STZ	37.4 ± 0.1	7.37 ± 0.02	41.5 ± 2.4
STZ + Caff	37.5 ± 0.1	7.39 ± 0.01	40.9 ± 0.9

Data are mean ± SEM of the following number of animals in each experimental group: control ( $n = 8$ ), caffeine-treated ( $n = 6$ ), STZ-treated ( $n = 6$ ) and STZ and caffeine-treated ( $n = 6$ ) rats.

USA). These physiology parameters were similar in the four experimental groups (Table 1). Plasma glucose concentration was quantified with the glucose oxidase method, using a multi-assay analyzer (GW7 Micro-Stat, Analox Instruments, London, UK).

### <sup>1</sup>H NMR spectroscopy and quantification of metabolites

All experiments were carried out using an INOVA spectrometer (Varian, Palo Alto, CA, USA) interfaced to an actively-shielded 9.4 T magnet with a 31 cm horizontal bore (Magnex Scientific, Abingdon, UK) using a homebuilt 10 mm <sup>1</sup>H quadrature surface coil. The rat brain was positioned in the isocentre of the magnet and fast-spin-echo images with repetition time of 5 s, echo time of 52 ms and echo train length of 8 were used to identify the hippocampus based on anatomical landmarks. Shimming was performed with FAST(EST)MAP (Gruetter and Tkáč 2000), and <sup>1</sup>H NMR spectra were acquired from a volume of interest (VOI) of 18 μL placed in the left hippocampus. SPECIAL with echo time of 2.8 ms and repetition time of 4 s (Mlynárik *et al.* 2006) was used for localization.

Spectral analysis was carried out using LCModel (Provencher, 1993) including a macromolecule spectrum in the database, as in previous studies (Mlynárik *et al.* 2006). The unsuppressed water signal measured from the same volume of interest was used as an internal reference for the quantification of the following 20 metabolites that constitute the neurochemical profile in the present study: glucose, ascorbate, phosphorylethanolamine, creatine, phosphocreatine, *myo*-inositol, taurine, *N*-acetylaspartate, aspartate, glutamate (Glu), glutamine, GABA, alanine, lactate, β-hydroxybutyrate, glycerophosphorylcholine phosphorylcholine, GSH, *N*-acetylaspartylglutamate, *scyllo*-inositol. The Cramér-Rao lower bound provided by LCModel was used as a measure of the reliability of the apparent metabolite concentration quantification (Cavassila *et al.* 2001). Metabolite concentrations with Cramér-Rao lower bound higher than 25% were not included in the analysis. Spectral quality was evaluated by analyzing the metabolite line with and signal to noise ratio that were provided by LCModel.

### Determination of glucose transport kinetics

The predominant transporter proteins (GLUT) involved in cerebral glucose utilization are GLUT1 and GLUT3, being GLUT1 present in all brain cells including the endothelial cells of the capillaries (with very low neuronal expression *in vivo*), and GLUT3 almost restricted to neurons (reviewed in Simpson *et al.* 2007). Thus,

GLUT1 is mainly responsible for the facilitative transport of glucose across the BBB. The model of glucose transport across the BBB was simplified to consider a three compartment system, as described in Gruetter *et al.* (1998): the BBB, which was considered to behave as a single transport step, separates the blood circulation compartment from the brain aqueous phase that is virtually separated from the metabolic pool where glucose is consumed. The transport across the BBB was described using Michaelis-Menten kinetics with unidirectional fluxes and symmetric kinetic constants for influx and efflux, and non-specific permeability of the BBB to glucose was excluded. Cerebral glucose consumption rate was assumed to be invariable over the range of glucose concentrations studied in all groups. Under the steady-state condition, the model of glucose transport is represented by the following mathematical equation:

$$\frac{dG_{\text{hipp}}}{dt} = T_{\text{influx}} - T_{\text{efflux}} - \text{CMR}_{\text{glc}} = 0 \quad (1)$$

In this equation,  $G_{\text{hipp}}$  is the glucose concentration in the hippocampus (in μmol/g),  $T$  is the rate of glucose influx or efflux across the BBB (in μmol/g/min), and  $\text{CMR}_{\text{glc}}$  is the cerebral metabolic rate for glucose consumption (in μmol/g/min).

Two types of enzymatic mechanism were considered for glucose transporters. First, the standard Michaelis-Menten model with the following expression relating hippocampal glucose to plasma glucose (see Gruetter *et al.* 1998):

$$G_{\text{hipp}} = V_d K_t \frac{\left(\frac{T_{\text{max}}}{\text{CMR}_{\text{glc}}} - 1\right) G_{\text{plasma}} - K_t}{\left(\frac{T_{\text{max}}}{\text{CMR}_{\text{glc}}} + 1\right) K_t + G_{\text{plasma}}} \quad (2)$$

$G_{\text{plasma}}$  is the plasma glucose concentration,  $T_{\text{max}}$  denotes the apparent maximal transport rate across the BBB (μmol/g/min),  $K_t$  denotes the apparent Michaelis-Menten constant (mM),  $V_d$  is the volume of the physical distribution space of glucose in the brain (0.77 mL/g).

Second, as at hyperglycemia the brain glucose approaches or even exceeds the  $K_t$  obtained with the standard Michaelis-Menten model (including observations in the present study), we used reversible Michaelis-Menten kinetics of glucose transport. Using this reversible model at steady state, the following equation expresses hippocampal glucose concentrations as function of plasma glucose and suggests a linear relation between the two variables as previously described (Gruetter *et al.* 1998):

$$G_{\text{hipp}} = V_d \frac{\left(\frac{T_{\text{max}}}{\text{CMR}_{\text{glc}}} - 1\right) G_{\text{plasma}} - K_t}{\frac{T_{\text{max}}}{\text{CMR}_{\text{glc}}} + 1} \quad (3)$$

For the estimation of the kinetic parameters of glucose transport at the BBB, glucose concentration in the hippocampus was calculated subtracting the contribution of plasma glucose in a blood volume of 3.4 mL for 100 g of cerebral tissue (Shockley and LaManna, 1988) from the total glucose signal in the <sup>1</sup>H NMR spectra.

### Hippocampal membrane preparations

After the NMR experiment, both hippocampi were readily dissected and stored at -80°C until membrane preparation for western blot analysis. Membranes from the whole hippocampus or from

Percoll-purified hippocampal synaptosomes were prepared as previously detailed (Duarte *et al.* 2006). Briefly, the two hippocampi from one rat were homogenized at 4°C in sucrose-HEPES buffer (composition 0.32 M sucrose, 1 mM EDTA, 10 mM HEPES, 1 mg/mL bovine serum albumin, pH 7.4). The resulting homogenate was centrifuged at 3000 *g* for 10 min at 4°C, the supernatant collected and centrifuged at 14 000 *g* for 12 min at 4°C. The pellet was re-suspended in 1 mL of a 45% (v/v) Percoll solution made up in Krebs-HEPES solution (composition in mM: 140 NaCl, 5 KCl, 10 HEPES, 1 EDTA, 5 glucose, pH 7.4). After centrifugation at 21 000 *g* for 2 min at 4°C, the top layer (nerve terminal fraction) was removed, washed and re-suspended in Krebs-HEPES solution. For total membrane preparation, a portion of the supernatant of the first centrifugation was taken, re-suspended in a solution of 50 mM Tris and 10 mM MgCl<sub>2</sub> (pH 7.4), centrifuged at 28 000 *g* for 20 min at 4°C, and the resulting pellet re-suspended in a Krebs-HEPES solution. An aliquot of each membrane preparation was saved for protein quantification using the bicinchoninic acid method (kit from Pierce Biotechnology, Rockford, IL, USA).

#### Western blot analysis

Western blot analysis was performed as previously described (Duarte *et al.* 2006). Briefly, each sample was diluted with five volumes of sodium dodecyl sulfate–polyacrylamide gel electrophoresis buffer containing 30% (v/v) glycerol, 0.6 M dithiothreitol, 10% (w/v) sodium dodecyl sulphate and 375 mM Tris-HCl pH 6.8, and boiled at 95°C for 5 min. These diluted samples (25 µg of protein amount) were separated by sodium dodecyl sulfate–polyacrylamide gel electrophoresis (7.5% separation gel topped with a 4% concentrating gel) under reducing conditions, together with pre-stained molecular weight markers (Biorad Laboratories, Amadora, Portugal), and then electro-transferred to polyvinylidene difluoride membranes (0.45 µm, from Amersham Biosciences, Buckinghamshire, UK). After blocking for 1 h at 21–25°C with 5% milk in Tris-buffered saline (Tris 20 mM, NaCl 140 mM, pH 7.6), containing 0.1% Tween 20 (TBS-T), the membranes were incubated overnight at 4°C with the primary antibodies against synaptophysin (dilution 1 : 10 000; from Sigma, Sintra, Portugal), synaptosome-associated protein of 25 kDa (SNAP25; dilution 1 : 10 000; from Sigma), syntaxin (dilution 1 : 10 000; from Sigma), post-synaptic density protein of 95 kDa (PSD95, dilution 1 : 20 000; from Chemicon, Temecula, CA, USA), microtubule-associated protein type 2 (MAP2; dilution 1 : 1000; from Santa Cruz Biotechnology, Frilabo, Portugal) or glial fibrillary acidic protein (GFAP; dilution 1 : 5000; from Sigma). After three 15 min washing periods with TBS-T containing 0.5% milk, the membranes were incubated with the alkaline phosphatase-conjugated anti-rabbit IgG or anti-mouse IgG secondary antibodies (dilution 1 : 10 000; from Amersham) in TBS-T containing 1% milk during 90 min at 21–25°C. After three 20-min washes in TBS-T with 0.5% milk, the membranes were incubated with enhanced chemi-fluorescent substrate (Amersham) and then analyzed with a VersaDoc 3000 system (Biorad).

The membranes were then re-probed and tested for  $\alpha$ -tubulin or  $\beta$ -actin immunoreactivity to confirm that similar amounts of protein were applied to the gels. Briefly, the membranes were incubated at 21–25°C for 30 min with 40% (v/v) methanol and 1 h with 0.1 M glycine buffer pH 2.3, and then blocked as previously described

before incubation with an anti- $\alpha$ -tubulin (dilution 1 : 10 000) or anti- $\beta$ -actin (dilution 1 : 5000) antibodies (both from Sigma) for 2 h at 21–25°C. The membranes were then washed, incubated with an anti-mouse IgG alkaline phosphatase-conjugated secondary antibody and analyzed as described above.

#### Quantification of serum insulin and caffeine

Insulin concentration was quantified by enzyme immunoassay using the Mercodia Ultrasensitive Mouse Insulin ELISA kit (Mercodia, Uppsala, Sweden), and the colorimetric endpoint measured in a SpectraMax Plus<sup>384</sup> spectrometer (Molecular Devices, Union City, CA, USA).

For caffeine measurement, each serum sample was added to an equal volume of methanol-acetone (4 : 1), mixed for 15 min, centrifuged at 3000 *g* for 15 min, and the supernatant saved for caffeine quantification. Samples (20 µL) were separated at 21–25°C using a reverse-phase column [LiChroCART 125 × 4 mm LiChrospher 100 RP-18 (5 µm) cartridge fitted into a ManuCART holder (Merck, Darmstadt, Germany)], using a Gilson system equipped with a UV detector set at 274 nm. The maximum peak in the absorption spectra of caffeine was confirmed in a 100 µM caffeine solution prepared in water-methanol (10 : 1), using a SpectraMax Plus<sup>384</sup> spectrometer. The eluent was 40% (v/v) methanol at pH 6.0 with a flow rate of 0.8 mL/min. The identification of the caffeine peak was performed by comparison of relative retention time with standard samples prepared in water-methanol-acetone (5 : 4 : 1) and its quantification achieved by calculating the peak areas then converted to concentration values by calibration with known standards ranging from 1 to 100 µM.

#### Statistics

Results are generally presented as mean ± SEM values of *n* experiments. Kinetic parameters of glucose transport  $K_t$  and  $T_{max}/CMR_{glc}$  were varied to achieve the best fit to the data, constraining  $K_t$  to take a positive value. Significant group differences were considered at  $p < 0.05$  in the statistical test. Student's *t*-test was used to compare the metabolic profile of controls and STZ-treated rats. ANOVA followed by the Bonferroni's post-test was used for comparison of multiple experimental groups.

#### Results

During the period when the rats had free to access caffeine, both before and after STZ-treatment, body weight and glycaemia were monitored. As shown in Fig. 1(a) and (b), after STZ injection, there was a reduction of weight gain and a significant sustained increase in pre-prandial glycaemia of the diabetic rats when compared to controls, whether the animals consumed caffeine or not. Caffeine consumption was not significantly different in control and STZ-treated rats ( $p > 0.05$ , Fig. 1c), leading to similar serum caffeine concentrations ( $p > 0.05$ , Fig. 1d). Serum insulin concentration was reduced in STZ-treated rats when compared to controls ( $p < 0.05$ ). Caffeine consumption did not affect significantly circulating insulin levels (Fig. 1e), suggesting that caffeine treatment did not interfere with STZ action.

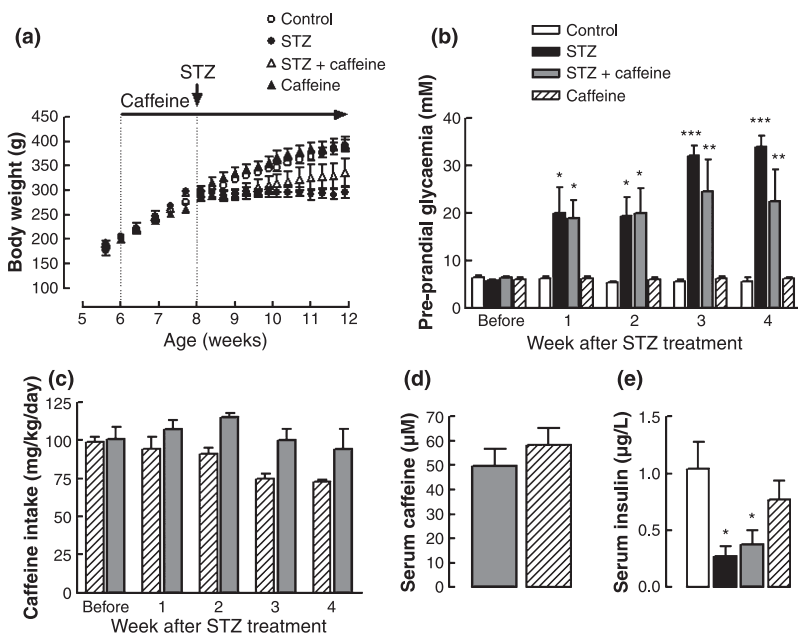


**Fig. 1** Characteristics of the animals used in the study, namely body weight (panel a), pre-prandial glycaemia (panel b), caffeine intake (panel c) measured across the housing period, and caffeine (panel d) and insulin (panel e) concentrations in the serum determined at the end of treatment. Caffeine (1 g/L) was provided in the drinking water from 6 weeks old onwards and STZ was administered at 8 weeks of age (a); these rats were maintained under hyperglycemia (b) and hypo-insulinemia (e) for 4 weeks. Data are mean  $\pm$  SEM of  $n = 6-8$  animals per experimental group. Significant differences of glycaemia (b) and serum insulin (e) were estimated with the ANOVA and are noted as follows: \* $p < 0.05$ , \*\* $p < 0.01$ , \*\*\* $p < 0.001$ , relative to control.

### Metabolite concentrations in the hippocampus

A detailed investigation of diabetes-induced alterations in the hippocampal metabolite concentrations under hyper- and normo-glycaemia was then carried out. Figure 2 shows typical  $^1\text{H}$  NMR spectra from the hippocampus obtained in the present study which illustrate the spectral quality achieved at high magnetic field, i.e. high spectral resolution with metabolite line width of  $7 \pm 1$  Hz and excellent signal to noise ratio of  $28 \pm 3$  in volumes as small as  $18 \mu\text{L}$  localized in the hippocampus.

When compared to controls at euglycaemia (plasma glucose of  $5.6 \pm 0.5$  mM,  $n = 8$ ), STZ-induced diabetic rats under hyperglycemia (plasma glucose of  $33.3 \pm 3.4$  mM,  $n = 6$ ) displayed significant alterations in the neurochemical profile (Fig. 3). Namely, there was an increase in the concentration of  $\beta$ -hydroxybutyrate, glycerophosphorylcholine, *myo*-inositol, *N*-acetylaspartate, taurine and total creatine, as well as a reduction of the concentration of GSH and *N*-acetylaspartylglutamate.

When glycaemia of STZ-treated rats was acutely normalized by insulin infusion, the majority of the metabolic alterations in the hippocampus returned to control levels (Fig. 3). In STZ-treated rats subjected to acute normalization of glycaemia (plasma glucose of  $7.9 \pm 1.7$  mM,  $n = 6$ ), the only significant change that remained was increased *myo*-inositol concentration ( $+36 \pm 5\%$ ,  $n = 6$ ,  $p < 0.01$  compared to controls). Interestingly, control rats under acute hyperglycemia did not exhibit significant alterations of the neurochemical profile, when compared to euglycaemia (data not shown), except for the expected increase in hippocampal glucose concentration.

Chronic caffeine consumption affected the neurochemical profile of STZ-induced diabetic rats (Fig. 4) in a particular way: the diabetes-induced increase of *myo*-inositol concentration was of lower amplitude, i.e. a  $15 \pm 5\%$  increase compared to controls ( $n = 6$ ,  $p < 0.05$ ); however, while the high taurine content in the hippocampus of STZ-treated rats was normalized at euglycaemia, it remained significantly increased in STZ-treated rats that consumed caffeine ( $+23 \pm 4\%$ ,  $n = 6$ ,  $p < 0.01$ , compared to controls). Importantly, the diabetes-induced combined increase of the concentration of taurine plus *myo*-inositol was not altered by caffeine consumption (Fig. 4). Finally, the other quantified metabolites that comprise the neurochemical profile were not significantly altered in the hippocampus of diabetic rats that consumed caffeine when compared to controls (data not shown).

In summary, the neurochemical profile in the hippocampus shows consistent modifications in *myo*-inositol and taurine concentrations caused by STZ-induced diabetes. Compared to control rats, diabetic rats under hyperglycemia displayed increased *myo*-inositol and taurine concentrations, and taurine levels were restored at euglycaemia. However, diabetic rats that consumed caffeine, showed smaller increase of *myo*-inositol content, and did not normalize diabetes-induced increment of taurine levels at euglycaemia.

### Hippocampal glucose transport

The hippocampal glucose concentration was significantly increased in the hippocampus of the diabetic rats, as visible in the glucose signal at 5.23 ppm in  $^1\text{H}$  NMR spectra, yet it approaches that of controls upon normalization of glycaemia (Fig. 2). As shown in Fig. 5, the dependence of hippocampal

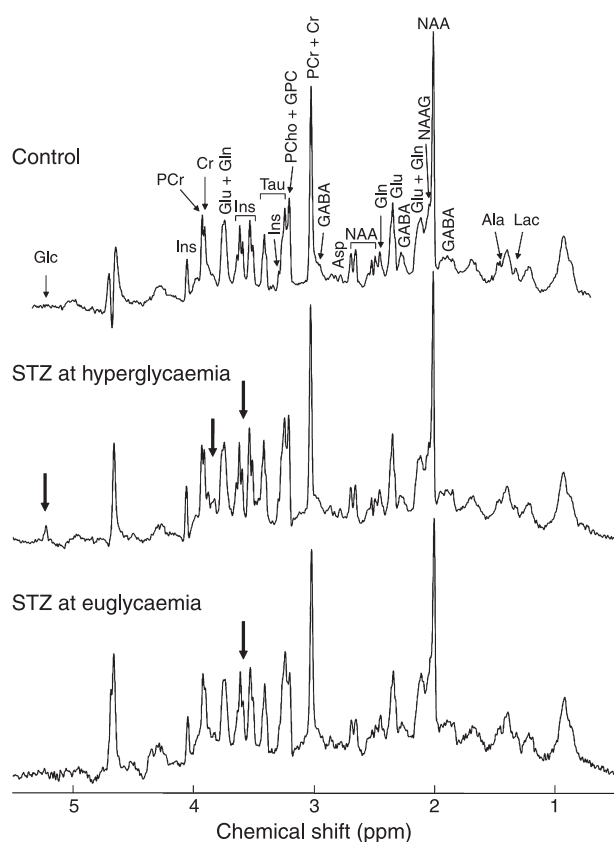


**Fig. 2** Representative *in vivo*  $^1\text{H}$  NMR spectra expanded from 0.5 to 5.5 ppm obtained in the hippocampus of 12 weeks old rats, either control (top spectrum) or STZ-induced diabetic at hyper- or euglycaemia (mid and bottom spectra, respectively). The bold arrows in the spectra from the hippocampus of STZ-induced diabetic rat emphasizes the increase in glucose and *myo*-inositol signals. The spectra were measured by the SPECIAL sequence with echo time of 2.8 ms, repetition time of 4 s, 640 scans and VOI of 18  $\mu\text{L}$  located in the hippocampus. For resolution enhancement, a shifted Gaussian function ( $gf = 0.12$  and  $gsf = 0.05$ ) was applied before Fourier transformation. Zero-phase but not baseline was corrected.

glucose on plasma glucose was not significantly different between controls and STZ-induced diabetic rats, suggesting that the rate of glucose transport across the BBB was not altered in the hippocampus in chronic hyperglycemia. This was further supported by similar kinetic parameters for glucose transport estimated with either the standard or reversible Michaelis-Menten models (Table 2). Likewise, caffeine consumption did not significantly affect glucose transport in the hippocampus of either control or STZ-treated rats (Fig. 5, Table 2).

### Synaptic alterations and astrogliosis in the hippocampus

Previous studies suggested the occurrence of synaptic degeneration upon a diabetic condition (Duarte *et al.* 2006; Grillo *et al.* 2005; Malone *et al.* 2006). In the present study,

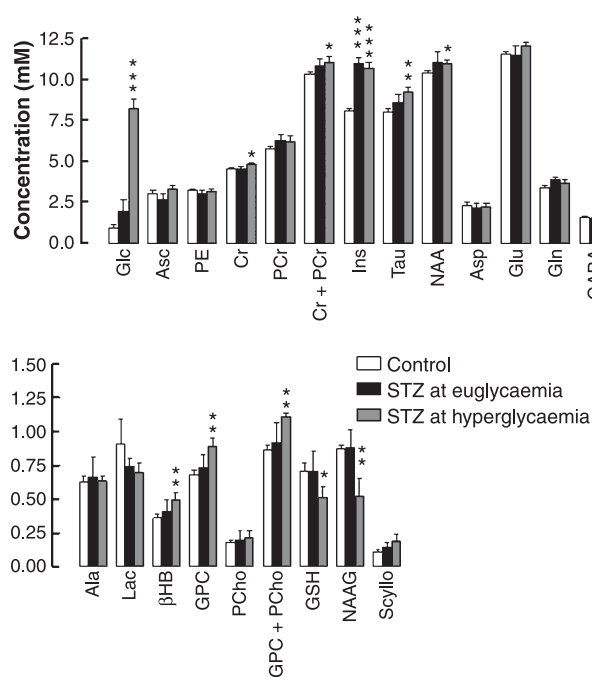


**Fig. 3** Effect of diabetes on the neurochemical profile of the hippocampus. The bar graphs show the concentrations of metabolites in the hippocampus of either STZ-treated rats at hyperglycemia (grey bars,  $n = 6$ ) and at euglycaemia (black bars,  $n = 6$ ), and age matched control rats (white bars,  $n = 8$ ), determined by  $^1\text{H}$  NMR spectroscopy. Data are mean  $\pm$  SEM and significance evaluated with the Student's *t*-test are noted as \* $p < 0.05$ , \*\* $p < 0.01$  and \*\*\* $p < 0.001$ , compared to control. Ala, alanine; Asc, ascorbate; Asp, aspartate;  $\beta\text{HB}$ ,  $\beta$ -hydroxybutyrate; Cr, creatine; Glc, glucose; Gln, glutamine; Glu, glutamate; GPC, glycerophosphorylcholine; Ins, *myo*-inositol; Lac, lactate; NAA, *N*-acetylaspartate; NAAG, *N*-acetylaspartatylglytamate; PCho, phosphorylcholine; PCr, phosphocreatine; PE, phosphorylethanolamine; scyllo, *scyllo*-inositol; Tau, taurine.

STZ-induced diabetic rats displayed reduced immunoreactivity for SNAP25 ( $-19.4 \pm 2.7\%$ ,  $p < 0.05$ ,  $n = 7$ ), synaptophysin ( $-17.4 \pm 2.2\%$ ,  $p < 0.05$ ,  $n = 5$ ) and syntaxin ( $-18.3 \pm 2.8\%$ ,  $p < 0.05$ ,  $n = 7$ ) in nerve terminal-enriched membranes of the hippocampus, when compared to controls (Fig. 6a–c). Furthermore, immunoreactivity of PSD95 was determined to evaluate the post-synaptic zone and was not significantly altered in nerve terminal membranes of STZ-treated rats when compared to controls ( $p > 0.05$ ,  $n = 5$ , Fig. 6d). Caffeine consumption prevented diabetes-induced reduction of synaptophysin and syntaxin, but failed to prevent the decrease of SNAP25 immunoreactivity. Caffeine intake did not affect significantly the immunoreactivity for any of these synaptic markers in nerve terminal membranes from the hippocampus of control rats. When compared to controls, STZ-induced diabetic rats failed to display altered MAP2 immunoreactivity ( $p > 0.05$ ,  $n = 5$ ) in total membranes from the hippocampus (Fig. 6e), suggesting preser-

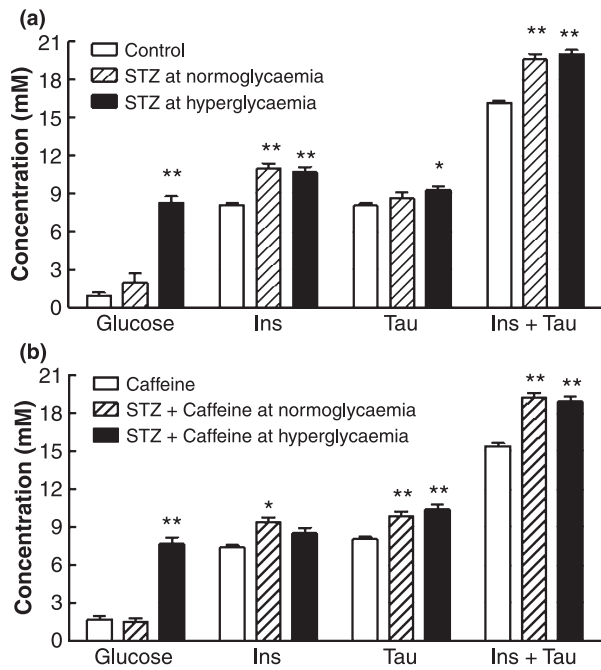


**Fig. 4** Caffeine consumption affected the relative concentrations of taurine and *myo*-inositol in the hippocampus of STZ-induced diabetic rats. Glucose, *myo*-inositol (Ins) and taurine (Tau) concentrations were determined by  $^1\text{H}$  NMR spectroscopy in the hippocampus of control and STZ-induced diabetic rats drinking water (panel a) or allowed to consume caffeine (1 g/L) through the drinking water for 6 weeks (panel b). Data are mean  $\pm$  SEM of 6–8 rats per experimental group and ANOVA (comparing the complete neurochemical profile) was used to gauge significance compared to the control group: \* $p < 0.05$ , \*\* $p < 0.01$ .

vation of the integrity of the neuronal structure beside the nerve terminal.

Several neurodegenerative disorders including diabetes induce astrogliosis (Baydas *et al.* 2003; Saravia *et al.* 2002). As shown in Fig. 6(f), hippocampal membranes from STZ-treated rats displayed increased immunoreactivity of GFAP relative to control rats ( $+19.6 \pm 4.7\%$ ,  $p < 0.05$ ,  $n = 8$ ). Caffeine consumption was devoid of effect on GFAP immunoreactivity in the hippocampus of control rats and prevented diabetes-induced increase in GFAP immunoreactivity ( $p > 0.05$ ,  $n = 8$ ), suggesting prevention of astrogliosis in the hippocampus.

## Discussion

In the present study, we found that chronic hyperglycemia, induced by STZ administration, caused a plethora of metabolic alterations in the hippocampus, most of which were normalized upon restoration of euglycaemia. Some of the metabolites more affected by hyperglycemia were *myo*-inositol, taurine and creatine, which are considered major

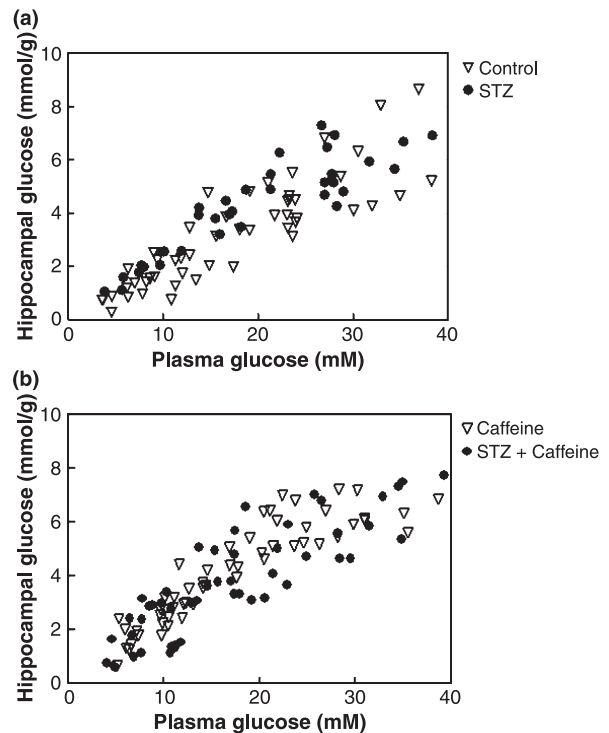


**Fig. 5** Caffeine consumption failed to affect glucose transport into the hippocampus. The graphs display the relationship between hippocampal and plasma glucose concentrations in control and STZ-treated rats drinking water (panel a) or allowed to consume caffeine (1 g/L) through the drinking water for 6 weeks (panel b). Data represent hippocampal glucose determined from  $^1\text{H}$  NMR spectra measured (during 40 min) after plasma glucose was stable for at least 15 min. Each experimental group consisted of 6–8 rats. The kinetic parameters of glucose transport were estimated from these data with either the reversible or the standard Michaelis-Menten model and are presented in Table 2.

organic osmolytes regulating brain osmotic adaptation (Lien *et al.* 1990, 1991), suggesting that such alterations of the neurochemical profile may be related to regulation of osmolarity. Although osmolarity regulation primarily relies on electrolytic balance, it is followed by a delayed response of organic osmolytes (Lien *et al.* 1991). Therefore, under chronic hyperglycemia the accumulation of organic osmolytes in the hippocampus is suitable to avoid ion-induced perturbation of protein function (Burg and Ferraris, 2008). Consistent with this, high concentration of *myo*-inositol has been reported in the hippocampus of Zucker diabetic fatty rats compared to controls (van der Graaf *et al.* 2004) and in the brain of diabetic patients relatively to healthy subjects (Geissler *et al.* 2003; Kreis and Ross, 1992). Also increased taurine transport (Trachtman *et al.* 1992) and concentration (Rose *et al.* 2000) had previously been reported in the brain of STZ-induced diabetic rats. Thus, the present results support the hypothesis that

**Table 2** Apparent Michaelis-Menten constant  $K_t$  and ratio of maximal transport rate ( $T_{max}$ ) to cerebral metabolic rate ( $CMR_{gluc}$ ) of glucose transport in the hippocampus, estimated with the reversible and standard Michaelis-Menten models

	Reversible model		Standard model	
	$K_t$ (mM)	$T_{max}/CMR_{gluc}$	$K_t$ (mM)	$T_{max}/CMR_{gluc}$
Control	1.23 (0.00–3.79)	1.77 (1.48–2.07)	7.77 (5.68–9.86)	3.11 (2.91–3.31)
STZ-treated	2.44 (0.00–5.41)	2.15 (1.82–2.51)	6.53 (4.91–8.26)	3.57 (3.27–3.86)
STZ and Caffeine-treated	0.49 (0.00–4.39)	1.98 (1.53–2.45)	6.41 (4.25–8.61)	3.64 (3.25–4.01)
Caffeine-treated	0.34 (0.00–1.58)	2.06 (1.77–2.34)	5.83 (4.41–7.25)	3.98 (3.64–4.31)

Kinetic parameters of glucose transport across the BBB were determined from the relationship between hippocampal and plasma glucose concentrations in each group of rats (data in Fig. 5). While the standard model was fitted to the whole range of plasma glucose concentrations, the reversible model was applied up to 20 mM. Data are mean (95% confidence interval).

hyperglycemia-induced hippocampal dysfunction mainly involves deregulation of osmotic balance rather than modification of primary metabolism.

Disruption of the BBB because of hyper-osmolarity has been proposed to occur in diabetic conditions, and particularly in STZ-induced diabetes (Huber *et al.* 2006). Such a disruption of the BBB is expected to increase BBB permeability and substantially increase brain glucose content, approaching plasmatic glucose content. This was not observed in the present study (see Fig. 5). In fact, there was a sustained glucose concentration gradient into the hippocampus, which indicates that increased leakage of glucose through a disrupted BBB did not occur in STZ-diabetic rats. Furthermore, it was observed that the rate of glucose transport across the BBB was not altered in the hippocampus of rats submitted to one month of chronic hyperglycemia. Likewise, previous studies in humans reported that poorly controlled diabetes did not affect brain glucose concentration (Sequist *et al.* 2005) or glucose transport and metabolism (Fanelli *et al.* 1998). This reflects a preservation of the capacity of the BBB to transport glucose relative to the glucose metabolic rate ( $T_{max}/CMR_{gluc}$ ) and could thus be affected by alterations in glucose metabolic rate. Together with the observation that [ $^{14}C$ ]glucose uptake and brain GLUT1 density were not altered in the hippocampus of STZ-treated rats (Simpson *et al.* 1999), our results support that glucose transport across the BBB is not affected by experimental diabetes. However, other studies reported that diabetes increased 2- [ $^{14}C$ ]deoxyglucose uptake in the dentate gyrus of the hippocampus without modification of GLUT1 or GLUT3 density (Duelli *et al.* 2000) or that brain glucose metabolism is reduced by chronic hyperglycemia (García-Espinosa *et al.* 2003). To what extent glucose metabolic rates are specifically altered at high plasma glucose concentrations or in chronic hyperglycemia (Pelligrino *et al.* 1992) remains to be determined. Interestingly, the present contention that chronic hyperglycemia does not affect glucose transport and content is the opposite of what was reported in chronic hypoglycemia (Lei and Gruetter, 2006), which suggests a differential regulation of GLUT1 gene

expression at the BBB in response to long-term alterations in glycaemia.

We found that chronic caffeine intake caused a very striking and particular effect on the neurochemical profile in the hippocampus, selectively affecting the level of osmolytes. In fact, caffeine consumption attenuated diabetes-induced increase of *myo*-inositol concentration, and increased the hippocampal levels of taurine, a cerebral osmolyte whose intracellular content changes in parallel with plasma osmolarity (Trachtman *et al.* 1992; Rose *et al.* 2000). These observations prompt the hypothesis that caffeine neuroprotection may also be related to this ability of caffeine to impact on osmotic adaptation of brain tissue. This effect of caffeine on taurine homeostasis in the hippocampus of diabetic rats may be related to the ability of adenosine receptors (the only known molecular targets of caffeine) to control osmotic swelling (Wurm *et al.* 2008) and taurine release from both neurons and glia (Hada *et al.* 1998). Thus, these effects of caffeine on diabetes-induced neurochemical profile are likely to be central effects, although caffeine consumption has been reported to have peripheral effects that may aid in the control of glucose homeostasis (van Dam and Hu 2005); however we observed that long-term caffeine intake failed to prevent hypoinsulinemia and hyperglycemia in STZ-treated rats, suggesting that these effects of caffeine on hippocampal metabolism are related to blockade of central adenosine receptors rather than peripheral actions of caffeine. However, it remains to be experimentally tested if this control of the levels of osmolytes is a direct effect on hippocampal tissue or if it results from indirect effect operated at the level of the hypothalamus, which is known to coordinate osmolar control of the body. It is tempting to speculate that this ability of caffeine to control the levels of osmolytes, namely of taurine may have a neuroprotective role in the hippocampus as taurine can also influence neurotransmission, interacting with inhibitory GABA<sub>A</sub>, GABA<sub>B</sub> or glycine receptors (reviewed in Albrecht and Schousboe, 2005), and modulating synaptic plasticity (del Olmo *et al.* 2000). In addition, taurine has antioxidant properties that

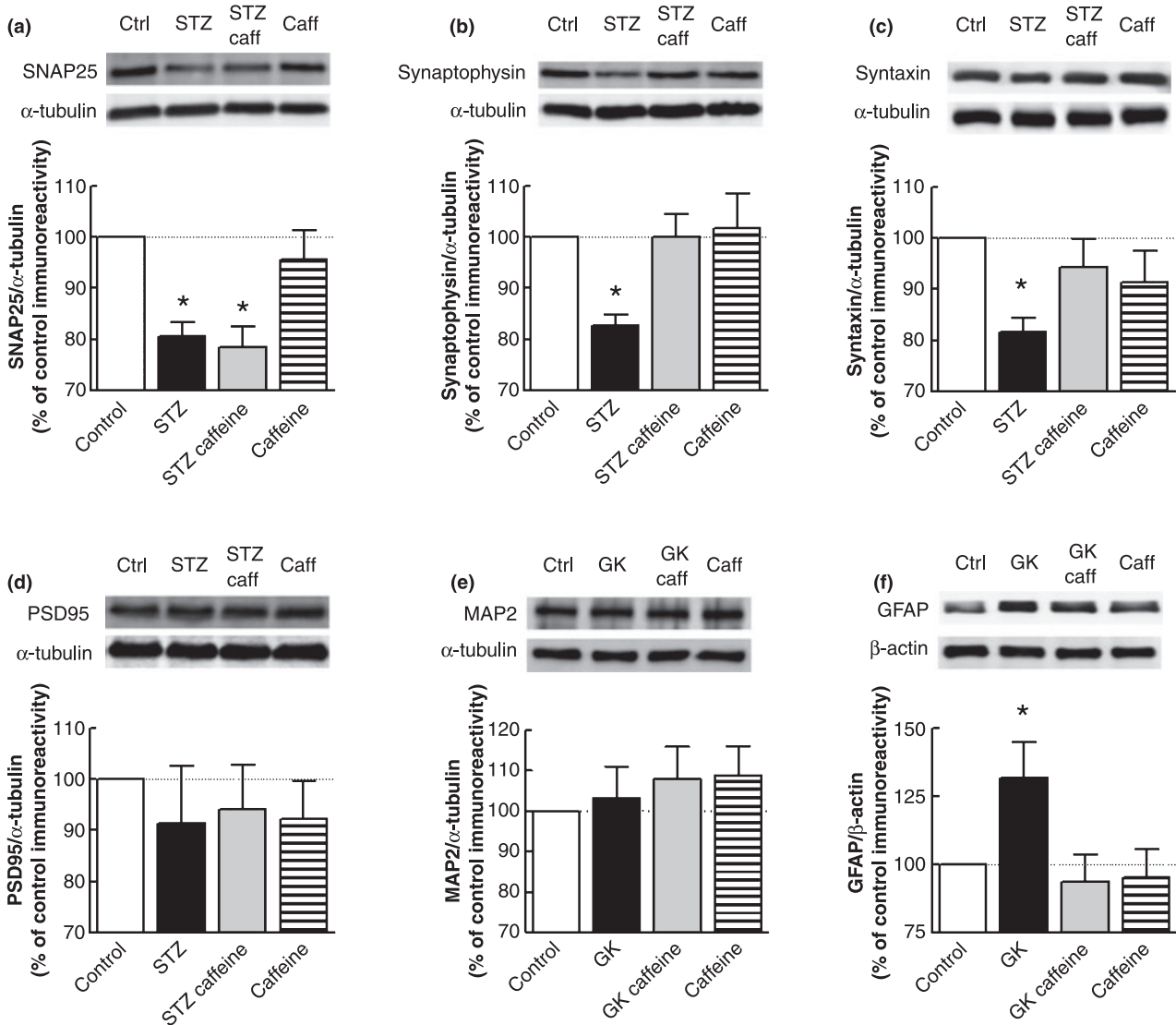


**Fig. 6** Caffeine consumption attenuates diabetes-induced synaptic degeneration and astrogliosis. Western blot analysis revealed that nerve terminal-enriched membranes from the hippocampus of STZ-induced diabetic rats displayed reduced immunoreactivity of SNAP25 (a), synaptophysin (b) and syntaxin (c) but not PSD95 (d), when compared to controls. Caffeine consumption prevented diabetes-induced reduction of synaptophysin and syntaxin but not SNAP25. Chronic hyperglycemia or caffeine consumption failed to affect MAP2 immunoreactivity in total membranes of the rat hippocampus (e). GFAP immunoreactivity was increased in total hippocampal membranes from STZ-induced diabetic rats (f), relative to control rats, which was prevented by caffeine consumption. Preparations from the

hippocampus of each animal (nerve terminal-enriched membranes for analysis of synaptic proteins or total membranes for MAP2 and GFAP) were applied in the SDS-PAGE gel (25 μg of protein). Immunoreactivities of synaptic proteins and MAP2 were normalized to α-tubulin and GFAP immunoreactivity was normalized to β-actin, being presented as percentage of control (open bars) in the same western blot experiment. In the graphs, black, gray and striped bars represent STZ-treated, STZ plus caffeine-treated and caffeine-treated control rats, respectively. Data are mean ± SEM of 5–8 experiments from different animals. \**p* < 0.05 compared to control using ANOVA followed by Bonferroni's post-test.

may contribute to reduce oxidative stress (Di Leo *et al.* 2004) caused by glucose neurotoxicity that occurs in diabetes (Tomlinson and Gardiner, 2008). In experimental models of diabetes, taurine was implicated in possible prevention of defects in nerve blood flow, motor nerve

conduction velocity, and nerve sensory thresholds (Li *et al.* 2006; Pop-Busui *et al.* 2001). However, it still remains to experimentally tested if the caffeine-induced modification of the taurine levels actually contribute for caffeine-induced neuroprotection in the diabetic hippocampus.

The present results show that STZ-treated rats display a pattern of neurodegeneration that does not affect the entire neuron, as suggested by unaltered immunoreactivity of the axonal marker MAP2, but is instead restricted to nerve terminals. This is in agreement with previous results showing that STZ-induced diabetes does not cause neuronal death (Bree *et al.* 2009; Grillo *et al.* 2005). Supporting this selective synaptic degeneration, it was observed that experimental diabetes caused a reduction of the density of synaptic proteins in the hippocampus, namely syntaxin, SNAP25 and synaptophysin. The density of the post-synaptic protein PSD95 was not significantly altered in the hippocampus of STZ-treated rats, when compared to the control rats, suggesting that diabetes mainly affects the pre-synaptic component of the synapse. Eventually, these modifications in nerve terminals may be responsible for the altered synaptic plasticity in the hippocampus and thus memory impairment observed in STZ-induced diabetic rats (Biessels *et al.* 1996). Remarkably, long-term caffeine consumption was able to prevent most synaptic alterations, except the reduction of SNAP25 density, in agreement with the proposed ability of caffeine to selectively prevent neuronal damage initiated by destruction of nerve terminals (Cunha *et al.* 2006; Silva *et al.* 2007). Furthermore, chronic hyperglycemia triggered astrogliosis in the hippocampus, as suggested by increased GFAP immunoreactivity in hippocampal membranes of STZ-induced diabetic rats, when compared to controls. This astrocytic proliferation might result from neuronal damage, as observed in other situations of neurodegeneration such as amyotrophic lateral sclerosis (Barbeito *et al.* 2004), Alzheimer's disease (Lauderback *et al.* 2001) and Lewy-body dementia (Honig *et al.* 2000). This astrogliosis may contribute for diabetes-induced hippocampal deterioration as reactive astrocytes are known to produce free radicals (Chao *et al.* 1996) and apoptotic factors (Crutcher *et al.* 1993; Ferrer *et al.* 2000, 2001). Caffeine intake prevented hyperglycemia-induced astrogliosis that was typified by increased GFAP immunoreactivity. These observations further strengthen the neuroprotective properties of chronic caffeine consumption against diabetic-induced neuropathy in the hippocampus.

In conclusion, it was found that glucose transport and content in the hippocampus were unaltered by chronic hyperglycemia. Thus, metabolic alterations in the hippocampus caused by STZ-induced diabetes are not related to changes in glucose transport through the BBB or alteration of the energy status. Otherwise, chronic hyperglycemia induced a number of changes in the neurochemical profile, possibly linked to osmolarity regulation that is essential for the maintenance of cellular homeostasis. Habitual caffeine consumption was able to prevent metabolic alterations in the diabetic hippocampus under chronic hyperglycemia, and it has a potential effect on the mechanisms of osmolarity regulation, modulating relative concentrations of *myo*-inositol and taurine metabolism, maintaining the total osmolyte

levels constant. This neuroprotective effect of caffeine was evident by its ability to prevent synaptic degeneration and astrogliosis caused by chronic hyperglycemia in STZ-induced diabetic rats. However, it remains to be addressed if this neuroprotection afforded by chronic caffeine consumption is accompanied by an amelioration of diabetes-induced hippocampal dysfunction.

## Acknowledgements

This work was supported by Fundação para a Ciência e a Tecnologia (Grant POCTI/SAU-NEU/56098/2004), Fundação Oriente and by Centre d'Imagerie BioMédicale (CIBM) of the UNIL, UNIGE, HUG, CHUV, EPFL and the Leenaards and Jeantet Foundations. João M. N. Duarte acknowledges a fellowship from Fundação para a Ciência e a Tecnologia, Portugal (SFRH/BD/17795/2004).

## Disclosure/conflict of interest

The authors declare there is no conflict of interest.

## References

- Albrecht J. and Schousboe A. (2005) Taurine interaction with neurotransmitter receptors in the CNS: an update. *Neurochem. Res.* **30**, 1615–1621.
- Alvarez E. O., Beauquis J., Revsin Y., Banzan A. M., Roig P., De Nicola A. F. and Saravia F. (2009) Cognitive dysfunction and hippocampal changes in experimental type 1 diabetes. *Behav. Brain Res.* **198**, 224–230.
- Barbeito L. H., Pehar M., Cassina P., Vargas M. R., Peluffo H., Viera L., Estévez A. G. and Beckman J. S. (2004) A role for astrocytes in motor neuron loss in amyotrophic lateral sclerosis. *Brain Res. Brain Res. Rev.* **47**, 263–274.
- Baydas G., Nedzvetskii V. S., Tuzcu M., Yasar A. and Kirichenko S. V. (2003) Increase of glial fibrillary acidic protein and S-100B in hippocampus and cortex of diabetic rats: effects of vitamin E. *Eur. J. Pharmacol.* **462**, 67–71.
- Biessels G. J., Kamal A., Ramakers G. M., Urban I. J., Spruijt B. M., Erkelens D. W. and Gispen W. H. (1996) Place learning and hippocampal synaptic plasticity in streptozotocin-induced diabetic rats. *Diabetes* **45**, 1259–1266.
- Brands A. M. A., Biessels G. J., de Haan E. H. F., Kappelle L. J. and Kessels R. P. C. (2005) The effects of type 1 diabetes on cognitive performance. *Diabetes Care* **28**, 726–735.
- Bree A. J., Puente E. C., Daphna-Iken D. and Fisher S. J. (2009) Diabetes increases brain damage caused by severe hypoglycemia. *Am. J. Physiol. Endocrinol. Metab.* **297**, E194–E201.
- Burg M. B. and Ferraris J. D. (2008) Intracellular organic osmolytes: function and regulation. *J. Biol. Chem.* **283**, 7309–7313.
- Cavassila S., Deval S., Huegen C., van Ormondt D. and Graveron-Demilly D. (2001) Cramér-Rao bounds: an evaluation tool for quantitation. *NMR Biomed.* **14**, 278–283.
- Chao C. C., Hu S., Sheng W. S., Bu D., Bukrinsky M. I. and Peterson P. K. (1996) Cytokine-stimulated astrocytes damage human neurons via a nitric oxide mechanism. *Glia* **16**, 276–284.
- Chen J. F., Sonsalla P. K., Pedata F., Melani A., Domenici M. R., Popoli P., Geiger J., Lopes L. V. and de Mendonça A. (2007) Adenosine A2A receptors and brain injury: broad spectrum of neuroprotec-

- tion, multifaceted actions and “fine tuning” modulation. *Prog. Neurobiol.* **83**, 310–331.
- Convit A., Wolf O. T., Tarshish C. and de Leon M. J. (2003) Reduced glucose tolerance is associated with poor memory performance and hippocampal atrophy among normal elderly. *Proc. Natl Acad. Sci. USA* **100**, 2019–2022.
- Crutcher K. A., Scott S. A., Liang S., Everson W. V. and Weingartner J. (1993) Detection of NGF-like activity in human brain tissue: increased levels in Alzheimer’s disease. *J. Neurosci.* **13**, 2540–2550.
- Cunha G. M., Canas P. M., Oliveira C. R. and Cunha R. A. (2006) Increased density and synapto-protective effect of adenosine A<sub>2A</sub> receptors upon sub-chronic restraint stress. *Neuroscience* **141**, 1775–1781.
- Cunha R. A. (2005) Neuroprotection by adenosine in the brain: from A<sub>1</sub> receptor activation to A<sub>2A</sub> receptor blockade. *Purinergic Signal.* **1**, 111–134.
- Cunha R. A. (2008) Caffeine, adenosine receptors, memory and Alzheimer disease. *Med. Clin. (Barc.)* **131**, 790–795.
- del Olmo N., Galarreta M., Bustamante J., Martín del Río R. and Solís J. M. (2000) Taurine-induced synaptic potentiation: role of calcium and interaction with LTP. *Neuropharmacology* **39**, 40–54.
- Di Leo M. A., Santini S. A., Silveri N. G., Giardina B., Franconi F. and Ghirlanda G. (2004) Long-term taurine supplementation reduces mortality rate in streptozotocin-induced diabetic rats. *Amino Acids* **27**, 187–191.
- Duarte J. M. N., Oliveira C. R., Ambrosio A. F. and Cunha R. A. (2006) Modification of adenosine A<sub>1</sub> and A<sub>2A</sub> receptor density in the hippocampus of streptozotocin-induced diabetic rats. *Neurochem. Int.* **48**, 144–150.
- Duelli R., Maurer M. H., Staudt R., Heiland S., Duembgen L. and Kuschinsky W. (2000) Increased cerebral glucose utilization and decreased glucose transporter Glut1 during chronic hyperglycemia in rat brain. *Brain Res.* **858**, 338–347.
- Fanelli C. G., Dence C. S., Markham J., Videen T. O., Paramore D. S., Cryer P. E. and Powers W. J. (1998) Blood-to-brain glucose transport and cerebral glucose metabolism are not reduced in poorly controlled type 1 diabetes. *Diabetes* **47**, 1444–1450.
- Ferrer I., Blanco R. and Carmona M. (2001) Differential expression of active, phosphorylation-dependent MAP kinases, MAPK/ERK, SAPK/JNK and p38, and specific transcription factor substrates following quinolinic acid excitotoxicity in the rat. *Brain Res. Mol. Brain Res.* **94**, 48–58.
- Ferrer I., Blanco R., Cutillas B. and Ambrosio S. (2000) Fas and Fas-L expression in Huntington’s disease and Parkinson’s disease. *Neuropathol. Appl. Neurobiol.* **26**, 424–433.
- Fredholm B. B., Bättig K., Holmén J., Nehlig A. and Zvartau E. E. (1999) Actions of caffeine in the brain with special reference to factors that contribute to its widespread use. *Pharmacol. Rev.* **51**, 83–133.
- García-Espinosa M. A., García-Martín M. L. and Cerdán S. (2003) Role of glial metabolism in diabetic encephalopathy as detected by high resolution <sup>13</sup>C NMR. *NMR Biomed.* **16**, 440–449.
- Geissler A., Frund R., Scholmerich J., Feuerbach S. and Zietz B. (2003) Alterations of cerebral metabolism in patients with diabetes mellitus studied by proton magnetic resonance spectroscopy. *Exp. Clin. Endocrinol. Diabetes* **111**, 421–427.
- Gold S. M., Dziobek I., Sweat V., Tirsi A., Rogers K., Bruehl H., Tsui W., Richardson S., Javier E. and Convit A. (2007) Hippocampal damage and memory impairments as possible early brain complications of type 2 diabetes. *Diabetologia* **50**, 711–719.
- Grillo C. A., Piroli G. G., Wood G. E., Reznikov L. R., McEwen B. S. and Reagan L. P. (2005) Immunocytochemical analysis of synaptic proteins provides new insights into diabetes-mediated plasticity in the rat hippocampus. *Neuroscience* **136**, 477–486.
- Gruetter R. and Tkác I. (2000) Field mapping without reference scan using asymmetric echo-planar techniques. *Magn. Reson. Med.* **43**, 319–323.
- Gruetter R., Ugurbil K. and Seaquist E. R. (1998) Steady-state cerebral glucose concentrations and transport in the human brain. *J. Neurochem.* **70**, 397–408.
- Hada J., Kaku T., Morimoto K., Hayashi Y. and Nagai K. (1998) Activation of adenosine A<sub>2</sub> receptors enhances high K<sup>+</sup>-evoked taurine release from rat hippocampus: a microdialysis study. *Amino Acids* **15**, 43–52.
- Hammer J., Qu H., Häberg A. and Sonnewald U. (2001) *In vivo* effects of adenosine A<sub>2</sub> receptor agonist and antagonist on neuronal and astrocytic intermediary metabolism studied with *ex vivo* <sup>13</sup>C MR spectroscopy. *J. Neurochem.* **79**, 885–892.
- Honig L. S., Chambliss D. D., Bigio E. H., Carroll S. L. and Elliott J. L. (2000) Glutamate transporter EAAT2 splice variants occur not only in ALS, but also in AD and controls. *Neurology* **55**, 1082–1088.
- Huber J. D., VanGilder R. L. and Houser K. A. (2006) Streptozotocin-induced diabetes progressively increases blood-brain barrier permeability in specific brain regions in rats. *Am. J. Physiol. Heart Circ. Physiol.* **291**, H2660–H2668.
- Kreis R. and Ross B. D. (1992) Cerebral metabolic disturbances in patients with subacute and chronic diabetes mellitus: detection with proton MR spectroscopy. *Radiology* **184**, 123–130.
- Lauderback C. M., Hackett J. M., Huang F. F., Keller J. N., Szveda L. I., Markesbery W. R. and Butterfield D. A. (2001) The glial glutamate transporter, GLT-1, is oxidatively modified by 4-hydroxy-2-nonenal in the Alzheimer’s disease brain: the role of Aβ1-42. *J. Neurochem.* **78**, 413–416.
- Lei H. and Gruetter R. (2006) Effect of chronic hypoglycaemia on glucose concentration and glycogen content in rat brain: a localized <sup>13</sup>C NMR study. *J. Neurochem.* **99**, 260–268.
- Li F., Abatan O. I., Kim H., Burnett D., Larkin D., Obrosova I. G. and Stevens M. J. (2006) Taurine reverses neurological and neurovascular deficits in Zucker diabetic fatty rats. *Neurobiol. Dis.* **22**, 669–676.
- Lien Y. H., Shapiro J. I. and Chan L. (1990) Effects of hypernatremia on organic brain osmoles. *J. Clin. Invest.* **85**, 1427–1435.
- Lien Y. H., Shapiro J. I. and Chan L. (1991) Study of brain electrolytes and organic osmolytes during correction of chronic hyponatremia. Implications for the pathogenesis of central pontine myelinolysis. *J. Clin. Invest.* **88**, 303–309.
- Malone J. I., Hanna S. K. and Saporta S. (2006) Hyperglycemic brain injury in the rat. *Brain Res.* **1076**, 9–15.
- McCall A. L., Millington W. R. and Wurtman R. J. (1982) Metabolic fuel and amino acid transport into the brain in experimental diabetes mellitus. *Proc. Natl Acad. Sci. USA* **79**, 5406–5410.
- Mlynárik V., Gambarota G., Frenkel H. and Gruetter R. (2006) Localized short-echo-time proton MR spectroscopy with full signal-intensity acquisition. *Magn. Reson. Med.* **56**, 965–970.
- Pelligrino D. A., LaManna J. C., Duckrow R. B., Bryan R. M. Jr and Harik S. I. (1992) Hyperglycemia and blood-brain barrier glucose transport. *J. Cereb. Blood Flow Metab.* **12**, 887–899.
- Pop-Busui R., Sullivan K. A., Van Huysen C., Bayer L., Cao X., Towns R. and Stevens M. J. (2001) Depletion of taurine in experimental diabetic neuropathy: implications for nerve metabolic, vascular, and functional deficits. *Exp. Neurol.* **168**, 259–272.
- Provencher S. W. (1993) Estimation of metabolite concentrations from localized *in vivo* proton NMR spectra. *Magn. Reson. Med.* **30**, 672–679.
- Rose S. J., Bushi M., Nagra I. and Davies W. E. (2000) Taurine fluxes in insulin dependent diabetes mellitus and rehydration in streptozotocin treated rats. *Adv. Exp. Med. Biol.* **483**, 497–501.

- Saravia F. E., Revsin Y., Gonzalez Deniselle M. C., Gonzalez S. L., Roig P., Lima A., Homo-Delarche F. and De Nicola A. F. (2002) Increased astrocyte reactivity in the hippocampus of murine models of type 1 diabetes: the nonobese diabetic (NOD) and streptozotocin-treated mice. *Brain Res.* **957**, 345–353.
- Seaquist E. R., Tkac I., Damberg G., Thomas W. and Gruetter R. (2005) Brain glucose concentrations in poorly controlled diabetes mellitus as measured by high-field magnetic resonance spectroscopy. *Metabolism* **54**, 1008–1013.
- Shockley R. P. and LaManna J. C. (1988) Determination of rat cerebral cortical blood volume changes by capillary mean transit time analysis during hypoxia, hypercapnia and hyperventilation. *Brain Res.* **454**, 170–178.
- Silva C. G., Porciúncula L. O., Canas P. M., Oliveira C. R. and Cunha R. A. (2007) Blockade of adenosine  $A_{2A}$  receptors prevents staurosporine-induced apoptosis of rat hippocampal neurons. *Neurobiol. Dis.* **27**, 182–189.
- Simpson I. A., Appel N. M., Hokari M., Oki J., Holman G. D., Maher F., Koehler-Stec E. M., Vannucci S. J. and Smith Q. R. (1999) Blood-brain barrier glucose transporter: effects of hypo- and hyperglycemia revisited. *J. Neurochem.* **72**, 238–247.
- Simpson I. A., Carruthers A. and Vannucci S. J. (2007) Supply and demand in cerebral energy metabolism: the role of nutrient transporters. *J. Cereb. Blood Flow Metab.* **27**, 1766–1791.
- Takahashi R. N., Pamplona F. A. and Prediger R. D. (2008) Adenosine receptor antagonists for cognitive dysfunction: a review of animal studies. *Front. Biosci.* **13**, 2614–2632.
- Tomlinson D. R. and Gardiner N. J. (2008) Glucose neurotoxicity. *Nat. Rev. Neurosci.* **9**, 36–45.
- Trachtman H., Futterweit S. and Sturman J. A. (1992) Cerebral taurine transport is increased during streptozocin-induced diabetes in rats. *Diabetes* **41**, 1130–1140.
- van Dam R. M. and Hu F. B. (2005) Coffee consumption and risk of type 2 diabetes: a systematic review. *JAMA* **294**, 97–104.
- van der Graaf M., Janssen S. W., van Asten J. J., Hermus A. R., Sweep C. G., Pikkemaat J. A., Martens G. J. and Heerschap A. (2004) Metabolic profile of the hippocampus of Zucker Diabetic Fatty rats assessed by *in vivo*  $^1\text{H}$  magnetic resonance spectroscopy. *NMR Biomed.* **17**, 405–410.
- Wurm A., Iandiev I., Hollborn M., Wiedemann P., Reichenbach A., Zimmermann H., Bringmann A. and Pannicke T. (2008) Purinergic receptor activation inhibits osmotic glial cell swelling in the diabetic rat retina. *Exp. Eye Res.* **87**, 385–393.